ENTE PER LE NUOVE TECNOLOGIE,
L'ENERGIA E L'AMBIENTE

Dipartimento Innovazione

BOOMERANG PROJECT: STRUCTURAL CALCULATIONS AND VERIFICATIONS OF THE MECHANICAL SUPPORT OF A SPACE CRYOGENIC SYSTEM

ALBERTO ZUCCHINI, ROBERTO ORSI
Centro Ricerche "Ezio Clementel", Bologna

RT/INN/95/18

Testo pervenuto nel dicembre 1995

SUMMARY

The "BOOMERANG" (Ballon Observations Of Millimetric Extragalactic Radiation ANd Geophysics) experiment is an international effort to measure the Cosmic Microwave Background anisotropy on angular scales of 20' to 4°, with unprecedented sensitivity, sky and spectral coverage. The telescope will be flown from Antarctica by NASA-NSBF with a long duration stratospheric balloon (1-3 weeks), and is scheduled for flight in 1996.
Space cryogenic systems need adequate mechanical support to survive the large accelerations and vibrations induced during launch and landing. Static and modal analyses were carried out in order to assist the design of the mechanical support of the space cryogenic system. This report describes the models and the results of the FEM analyses carried out for different design solutions (kevlar cords or fiber-glass cylinders) of the cryostat support structure.

RIASSUNTO

L'esperimento "BOOMERANG" consiste in uno sforzo internazionale volto a misure di anisotropia della radiazione di fondo cosmico su scala angolare fra 20' e 4°, con sensibilita', copertura spaziale e spettrale senza precedenti. Il telescopio verra' lanciato dalla NASA-NSBF con un pallone stratosferico per una missione di lunga durata (1-3 settimane) ed il lancio e' programmato nel 1996.
I sistemi criogenici spaziali necessitano di adeguato supporto per superare le elevate accelerazioni e vibrazioni indotte durante le fasi di lancio e di atterraggio. Analisi statiche e modali sono state eseguite al fine di fornire utili elementi di valutazione per la progettazione del supporto meccanico del sistema criogenico spaziale. Nel presente rapporto si descrivono i modelli ed i risultati dell'analisi FEM effettuata per diverse soluzioni progettuali (cavi Kevlar o cilindri di vetronite) del criostato.

Contents

1.0 Introduction

The "BOOMERANG" (Balloon Observations of Millimetric Extragalactic RAdiation ANd Geophysics) experiment [1] is an internationally effort to measure the Cosmic Microwave Background (CMB) anisotropy on angular scales of 20' to 4°. The telescope will be flown from Antarctica by NASA-NSBF with long duration stratospheric balloon (1-3 weeks) and is scheduled for flight in 1996. Why from Antarctica? There are two unique features of Antarctic Ballooning which make it very attractive for CMB anisotropy experiments. The first one is the flight duration. Extensive tests made by NASA-NSBF have shown that stratospheric balloons launched from latitudes $\cong -80°$ travel along the meridian, coming back to the launch site in 7-20 days. That has to be compared to about 1 day flights available from temperate latitudes. The second feature is that the launch campaign is performed during the Antarctic summer (December and January) and a region with very low Galactic dust contrast is available in the anti-sun direction.
The experiment is designed to produce an image of the Cosmic Microwave Background with high sensitivity and large sky coverage. These data will tightly constrain the baryon density, the reionisation history and the formation of large scale structure in the universe.
BOOMERANG will test technologies and return science data that are essential to the design of a future space-borne mission to map CMB anisotropy.
This report describes the models and the results of the FEM analyses performed on the mechanical support of the cryostat which is a component of the equipment. Space cryogenic systems need adequate mechanical support to survive the large accelerations and vibrations induced by launch and landing. Landing is the most critical condition: the maximum stress is reached during landing at the time of full parachute opening when the structure undergoes an upward acceleration, estimated to 10g.
Vibrations may be critical for both the structure and the equipment. Thus it is important to evaluate the natural frequencies of the cryostat in order to avoid undesirable resonance effects.
Two different proposed approaches to the design of the support of the cryogenic system (kevlar cords or fiber-glass cylinders) have been studied in order to produce as much information as possible in the choice of an adequate final solution.
The calculations have been performed with Finite Element Code ABAQUS [2].

2.0 The Instrument

The main components of the experiments are (figg. 1-3) :
- an off-axis 1.2 m telescope;
- a 4-band x 8 pixel bolometric receiver;
- an alt-azimuth gondola with reaction wheel pointing capability.

The instrument has been specially designed to overcome problems typical of Antarctic ballooning: the long flight duration forces the designer to use special cryogenic systems; the enhanced cosmic rays flux in polar regions involves the use of special bolometers; the presence of the sun allows the use of solar panels for power supply but also forces the use of multiple sun shields for good thermal performance of the system. The ballon is far from the ground equipment, so special data collection/telemetry systems have to be used, and interactivity with the system is reduced. The concept for the experiment is shown if fig.3.
This report will focus the attention on the cryostat, which was developed in ENEA-Frascati and at the University of Rome, and in particular on its supporting system.

2.1 General Description of the Cryostat

An essential scheme of the cryostat is shown in fig.4 and the main components are evidenced in fig.5. The long duration cryostat consists of a main container (1) supported by 4 square sectioned bars (2) with two attachment points (A, B) for each bar, of a 70 liter liquid N_2 tank and of a 40 liter He tank.
In more detail, liquid N_2 is confined between two containers (5, 6) which are supported by an upper ring fixed to a flange (3) and by a lower ring connected to a flange (4) with kevlar cords. This complicated supporting system assures the high thermal insulation, which is essential for a long duration experiment.
The liquid He torus (7) is similarly fixed. Its supporting system (8) is shown in fig.6 and consists of six steel bars jointed at their bolted ends to an upper ring and to a lower one. Two kevlar cords fix the liquid He container to this structure. The optical instruments are borne by the same supporting system as for the liquid He torus and are located in the cylindrical volume delimited by the inner radius of the liquid He torus.
A cylindrical thermal shield with no structural function located very close to the outer wall of the liquid He torus (7) has not been represented in fig.5 for the sake of clearness.
All the containers and the structural components, with the exception of the six internal steel bars (8) and of the supporting kevlar cords, are made with ANTICORODAL G.

2.2 Purpose of the Analyses

The purposes of the analysis are:
1) the stress distribution in the cryostat supporting system under the most severe loading condition, with particular reference to:
   - the main container ((1) in fig.5);
   - the four square sectioned bars ((2) in fig.5);
   - the upper supporting ring ((3) in fig.5),

   Such a condition is reached during landing at the time of the full parachute opening, when the structure undergoes the maximum upward acceleration which has been estimated to 10 g.
2) the most significant natural frequencies and the corresponding mode shapes of the suspended cryostat, that is all the masses supported by the kevlar cords.

During the design process, the instrument has been modified several times and the final design may substantially differ from the ones considered in the analyses.

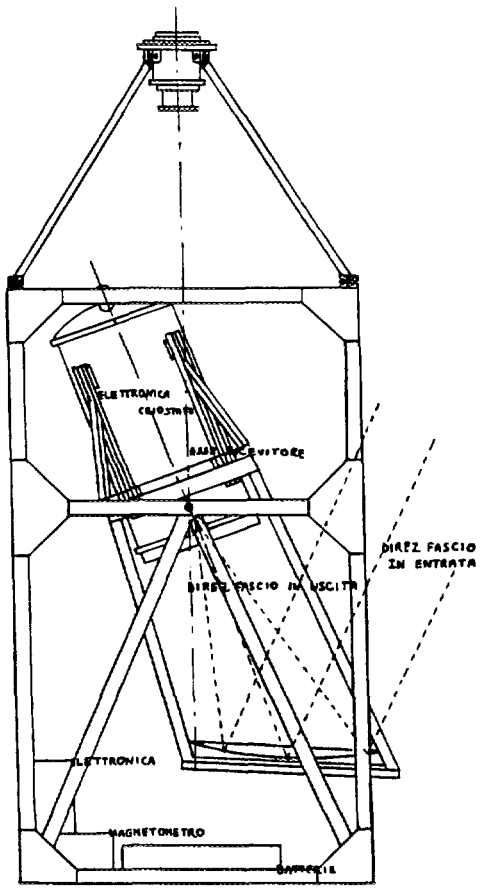

fig. 1

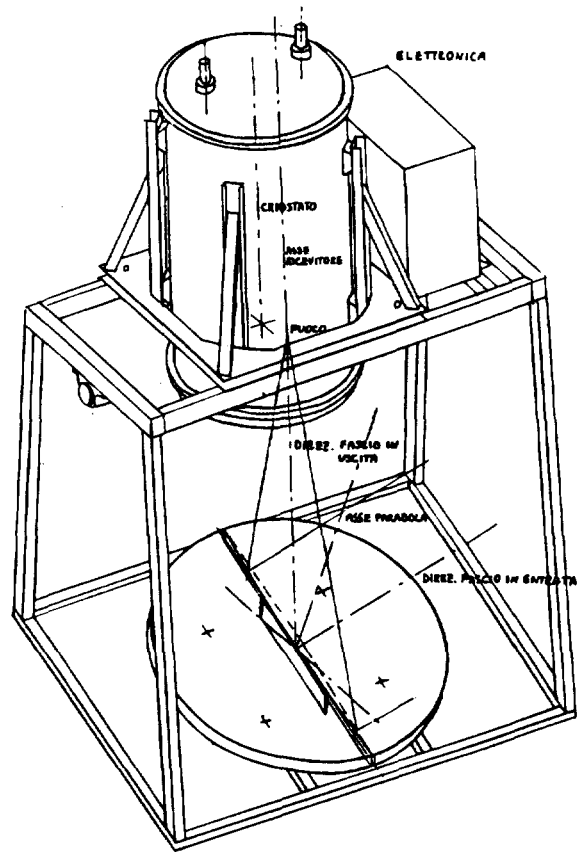

fig. 2

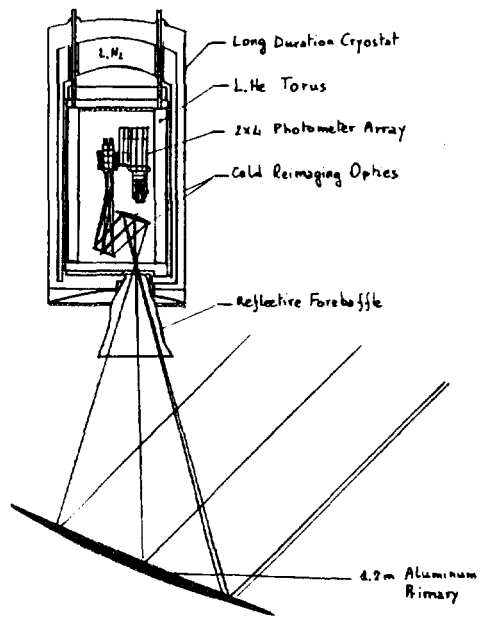

fig. 3

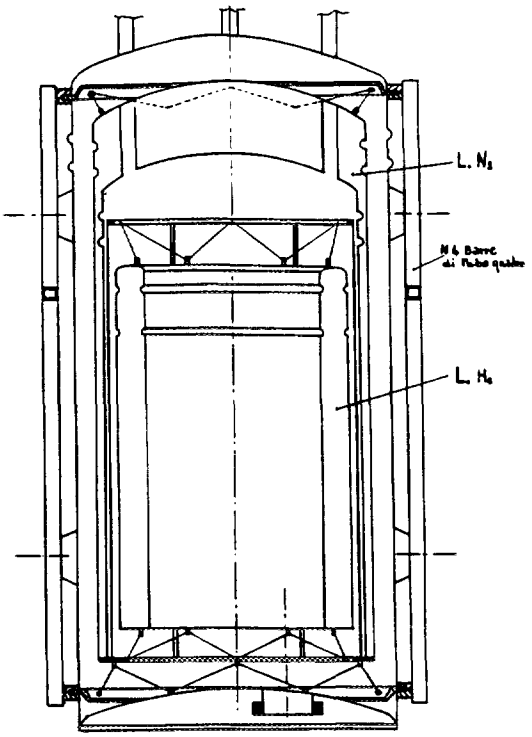

fig. 4

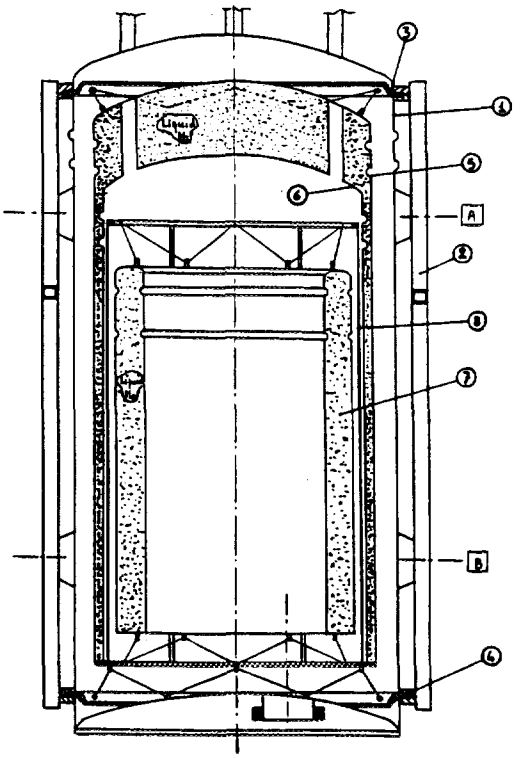

fig. 5

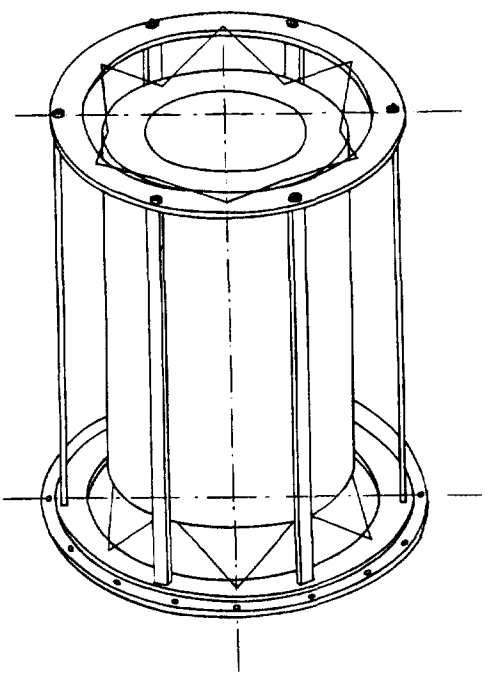

fig. 6

2.3 Materials

Material properties assumed in the analysis :

- ANTICORODAL G (Al Si_2 Mn Mg , UNI 3055)

ρ [mass density] = 2710. [kg / m^3]
E [Young's modulus] = 70.0 [GPa]
υ [Poisson's ratio] = 0.3 (value assumed in the calculations)

- KEVLAR 29

E [Young's modulus] = 29. [GPa]
υ [Poisson's ratio] = 0.3
ρ [mass density] = 1440. [kg / m^3]

- FIBER GLASS

E [Young's modulus] = 25. [GPa]
υ [Poisson's ratio] = 0.3
ρ [mass density] = 1950. [kg / m^3]

3.0 Static Calculations

As it was mentioned in par 2.2, the most severe loading condition happens as soon as the parachute opening has been completed, and it has been estimated, according to previous experiences, to 10 times the gravity force.
Even though this is a dynamic load, the maximum stresses and deformations were evaluated by a static simulation with the maximum force on the upper ring due to inertial effects equal to 10 times the natural weight of the suspended masses. Thus the static load, simulating the maximum dynamic load, has been applied to the sole upper ring of the supporting system in the direction of the kevlar cords (in normal operative conditions) without any need of modelling the suspended structure. It is worth while mentioning as for the static load, that the deformed configuration has been supposed not to introduce significant variations of the loading directions with respect to those in the undeformed status.

3.1 Geometric Data

The reference design with its related dimensions in [mm] for the static analysis is shown in fig.7. A scheeme of the kevlar cord arrangement at the upper ring to support the internal components is shown in fig.8a, where:

$R = 315$ [mm]

$r = 264$ [mm]

$\delta = 50$ [mm]

kevlar cord diameter = 3.2 [mm]

3.2 Loads

The masses of the main components of the structure with their related accessories, and of the equipment can be summarized as follows:

Liquid N_2 container :	38	[kg]
Liquid He torus :	14	[kg]
He thermal shield :	8	[kg]
Upper and lower rings :	4	[kg]
Optical equipment :	15	[kg]
Liquid N_2 :	49	[kg]
Liquid He :	8.5	[kg]
Total suspended mass :	136.5	[kg]
Outside container :	47	[kg]

Because of the symmetry of the structure and of the loads, it is possible to consider only one quarter of the model as it is shown in fig.8.
By taking into account what mentioned in the previous paragraphs, the tension T in the cord and the forces exerted at points A and B of the upper ring by the cord (fig.8b) can easily be calculated by simply imposing force equilibrium and symmetry conditions in the undeformed geometric configuration.

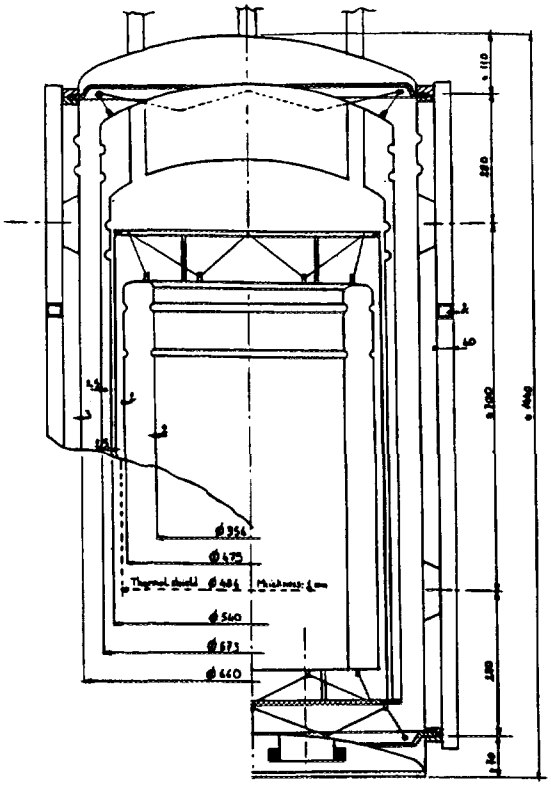

fig. 7

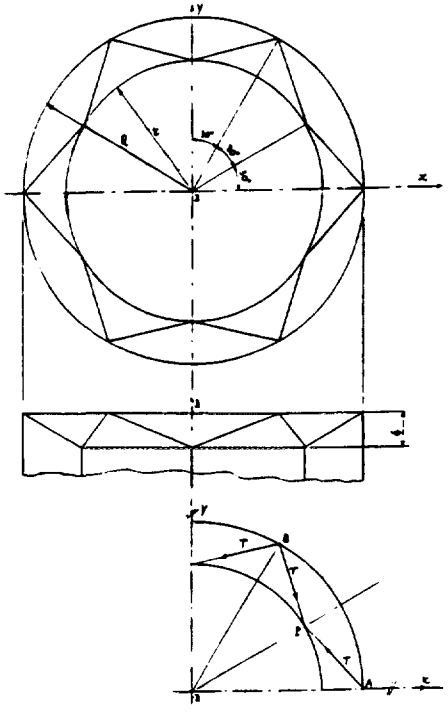

fig. 8 a

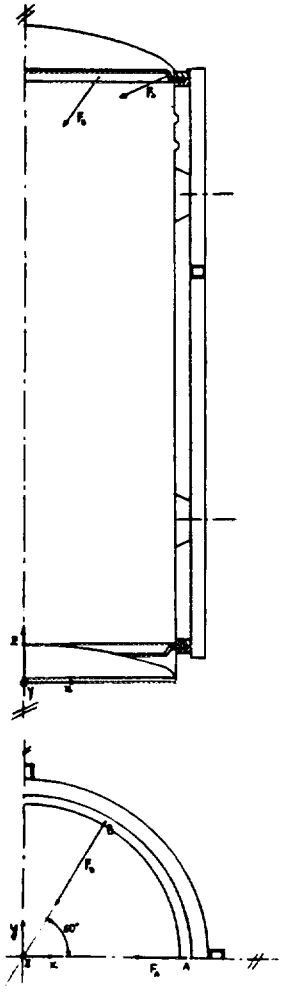

fig. 8 b

The total load P (directed along z) supported by the upper ring is:

$P = 136.5 * 10\ g \cong 13400\ [N]$

By imposing equilibrium of forces along z (vertical direction) and since there are 6 supporting points on the ring, we get after replacing the geometric values reported in par 3.1 :

$$T = \frac{P}{2 \cdot 6} \frac{\sqrt{r^2 + R^2 + \delta^2 - 2rR\cos 30°}}{\delta} \cong 3700\ [N]$$

$$F_{Ax} = -\frac{P}{2 \cdot 6} \frac{(R - r\cos 30°)}{\delta} = -1929\ [N] \quad \text{(radial direction)}$$

$$F_{Ay} = 0$$

$$F_{Az} = -\frac{P}{2 \cdot 6} = -1117\ [N]$$

$$F_{Bx} = -\frac{P}{6} \frac{(R - r\cos 30°)}{\delta} \cos 30° = -3341\ [N]$$

$$F_{By} = -\frac{P}{6} \frac{(R - r\cos 30°)}{\delta} \sin 30° = -1929\ [N]$$

$$F_{Bz} = -\frac{P}{6} = -2233\ [N]$$

In addition to these concentratd forces, a distributed load has been supposed to act on the supporting system equal to 10 times its natural weight.

3.3 Finite Element Models

The outside container has been simulated by two different finite element models (fig.9a,b) in order to assess the reliability of the results in the most stressed zone, that is in the neighbourhood of the load application points.
Only one quarter of the structure has been simulated because of symmetry.
The less refined model consists of 176 quadratic elements, 679 nodes, 4074 degrees of freedom (dofs), whereas the more refined one has 224 quadric elements, 887 nodes and 5322 dofs.
The wall, the bottom and the top of the main container have been simulated by shell elements.
Beam elements have been used to model both the upper and the lower flanges, the related supporting rings and the external supporting bars. More precisely, the upper ring and the related flanges have been simulated by a unique set of beams with cross section equal to the sum of the corresponding ones (fig.10a). The cross section of the beams simulating the lower ring and the related flanges is shown in fig.10b.
The material density of the outside container has fictitiously been modified from 2710 $[kg/m^3]$ to 3215 $[kg/m^3]$ in order to take into account the weight of the unmodelled details of the structure.
Different boundary conditions have been imposed in order to evaluate the influence and the effects of constraints on the static response of the structure to the previously described loading conditions. More precisely the following cases have been studied:

case a : less refined mesh (fig.11a)
Each bar supporting the cryostat has been connected to the outside container by six rigid beams and has been clamped at two nodes in correspondence of the connection with the supporting frame.

case b : less refined mesh (fig.11b)
There are the same boundary conditions as for case a, but the lower clamped nodes are located higher then in case a.

case c : more refined mesh (fig.11c)
There are the same boundary conditions as for case a.

case d : more refined mesh (fig.11d)
Each bar supporting the cryostat has been connected to the outside container by six pinned rigid links between nodes (to restrain displacements only) instead of rigid beams. The clamped nodes are the same as in case a.

case e : more refined mesh (fig.11e)
There are the same boundary conditions as for case a, but the top and bottom rigid beams between the container and the supporting bars have been removed.

3.4 Results

The main results of the analyses are summarized in Tab.1 (maximum Von Mises stress) and in Tab.2 (maximum displacements in absolute value).
Each analysis has been identified according to the classification described in 3.3.
The highest stress and displacement values are located in the loaded area of the container in all cases, with the only exception of case e as for displacements along x and y. In this case such displacements are maximum at the top of the two supporting bars, since the rigid beam links between the container and both ends of the supporting bars are missing.
As it can easily be noticed, the maximum stress values which have been calculated are quite below the resistence limits of the alluminum alloy employed for the cryostat (Anticorodal yield stress $\sigma_y = 196 \div 245$ Mpa).
The deformed shapes respectively of cases a, c, d, e are shown in fig.12.

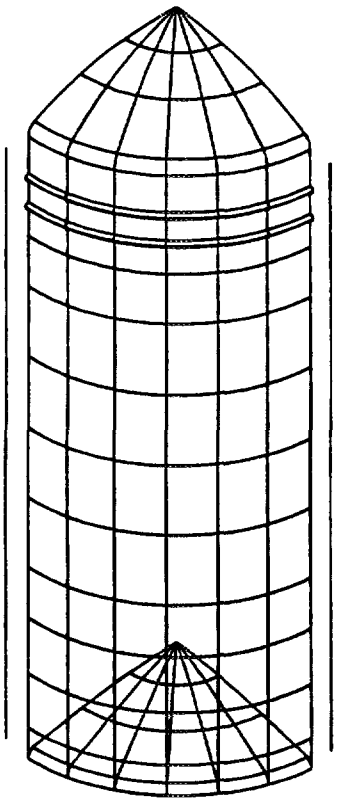

fig. 9 a

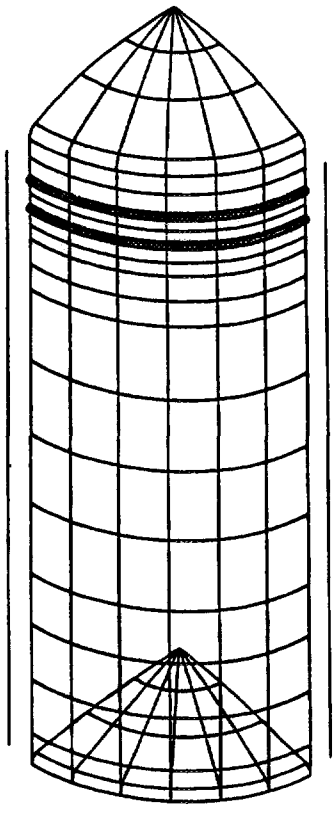

fig. 9 b

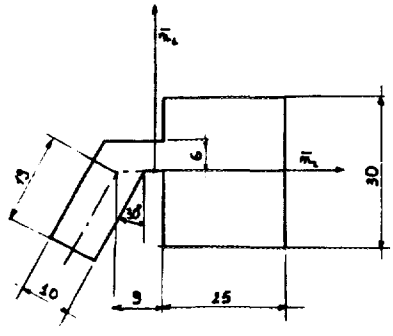

fig. 10 a

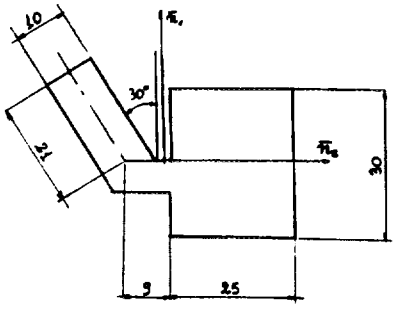

fig. 10 b

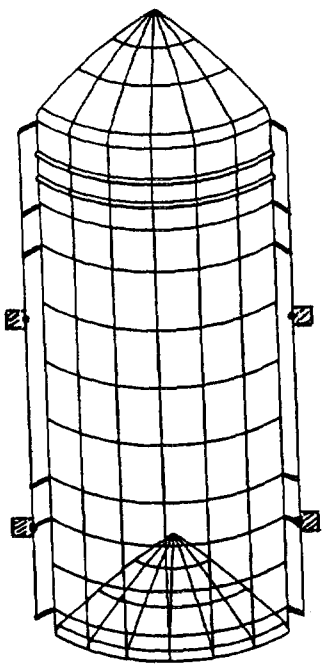

case **a**

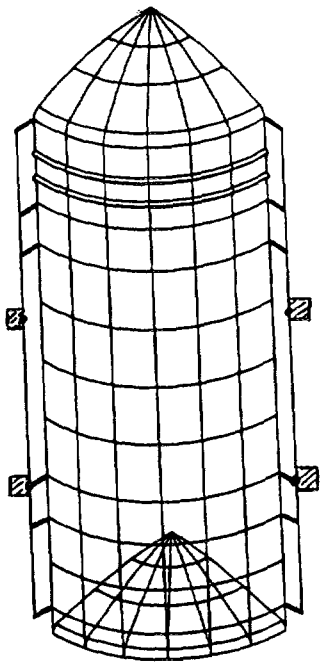

case **b**

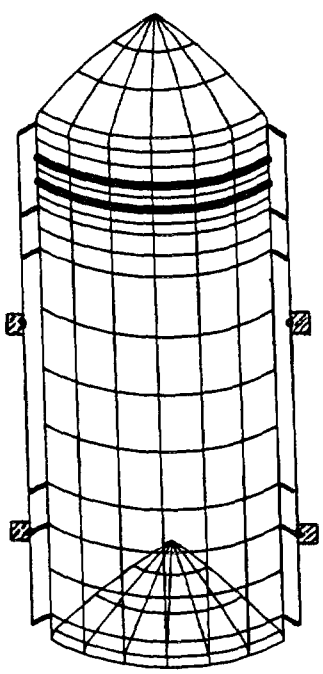

case **c**

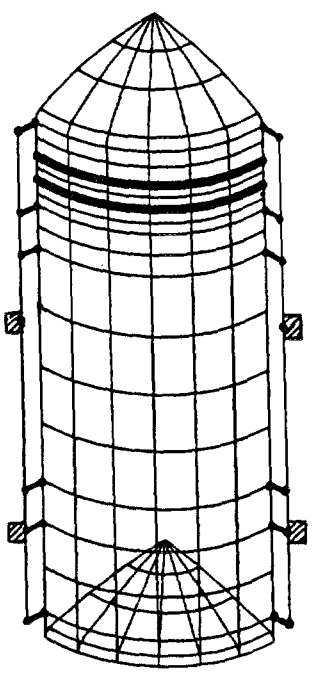

case **d**

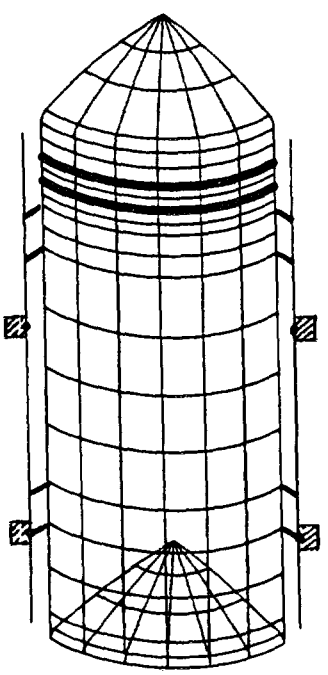

case **e**

fig. 11

Tab.1 Maximum Von Mises Stress [MPa]

Case	Container	Supporting bar ($\Phi = 0°$)	Supporting bar ($\Phi = 90°$)	Upper ring
a	33.7	11.7	10.6	13.3
b	33.7	11.6	10.2	13.3
c	36.9	11.8	10.6	13.5
d	40.4	0.8	1.5	13.7
e	39.8	8.6	9.8	14.0

Tab.2 Maximum Displacement [mm]

Case	|Dx|	|Dy|	|Dz|
a	0.06	0.08	0.09
b	0.06	0.08	0.09
c	0.06	0.09	0.09
d	0.09	0.09	0.13
e	0.27	0.28	0.12

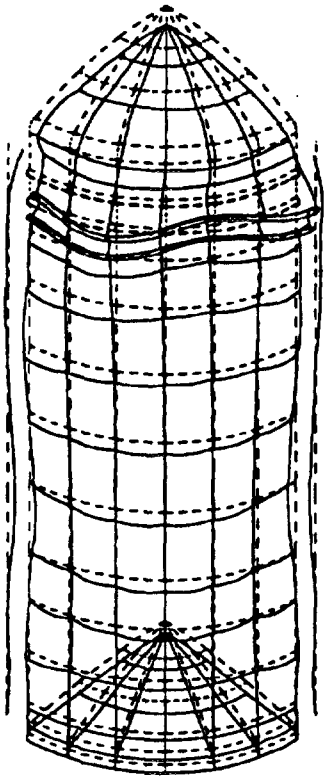

case **a**

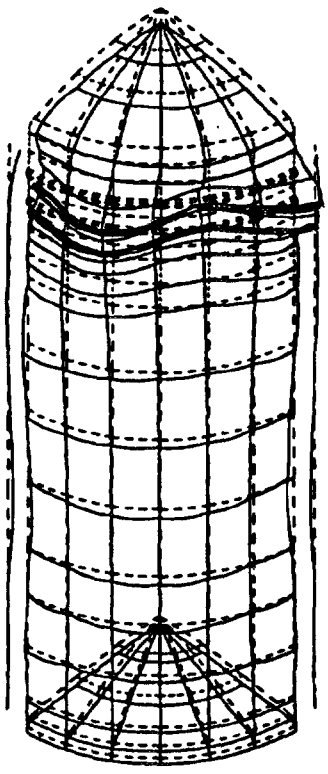

case **c**

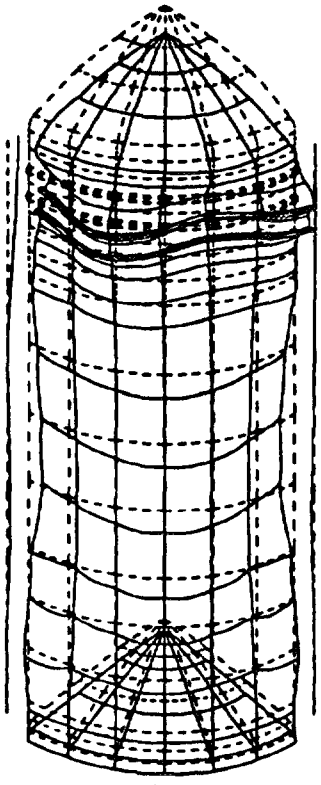

case **d**

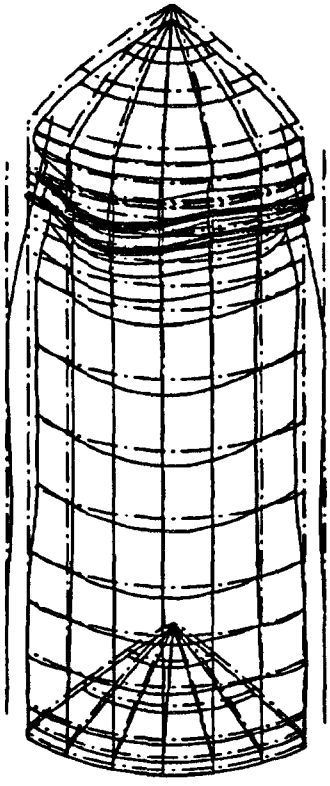

case **e**

fig. 12

4.0 Modal Analysis

The mechanical design of the cryostat support system is aimed to provide structural strength during launch and landing and to reduce noise by induced vibrations during measurements. Thus it is required to analyze the lowest natural frequencies of the system and the corresponding mode shapes.
Some simplified hypotheses have been introduced in the development of a finite element model adequate to this purpose.

4.1 Input Data and Model

The geometrical features of the cryostat assumed for the modal analysis are summarized in fig.13, where all the dimensions are expressed in [mm].
With respect to static analysis, the external supporting bars and the outside container have been neglected because much stiffer than the supporting system of the suspended structure, that is the kevlar cords having a diameter of 3.2 [mm]. Each kevlar cord connecting the cryostat to the upper and lower rings can be simulated by a set of 12 springs connected to the external N_2 container at one end and clamped at the other end.
The structure to be analyzed consists of:

- the external and internal anticorodal tanks for liquid N_2, which is confined among these two containers and a bottom anticorodal plate 8 [mm] thick;
- the supporting system of the He container consisting of 6 steel bars located at a regular angular interval of 60°, fixed to the bottom anticorodal plate and interconnected at their top by an anticorodal ring;
- the He container connected at the top and at the bottom to the supporting frame by kevlar cords having a diameter of 3.2 [mm] and each of them simulated as a set of 12 springs. The toroidal He container is much stiffer than its supporting system and has been simulated by a rigid link of the 12 springs to a fictitious lumped mass with equivalent inertial properties.

The properties of the materials employed in the model are reported in par. 2.3.
The following masses are simulated in the FEM model:

Liquid N_2 containers :	38	[kg]
Liquid N_2 :	60	[kg]
Liquid He container :	14	[kg]
Liquid He :	9	[kg]
Thermal shield :	8	[kg]
Optical equipment :	15	[kg]
Kevlar cords + supporting frame + anticorodal plate :	13	[kg]
TOTAL MASS:	157	[kg]

The mass density of the external and internal N_2 containers has been artificially increased from 2710 [kg / m^3] in order to take into account the right inertial effects of the two tanks. That is due to liquid N_2, structural details and pertinent equipment that have been neglected while modelling, because they are not significant from the stiffness point of view. Anyhow their inertial effects cannot be ignored.
Liquid N_2 mass has been distributed on the two tank structural volumes as follows:

- 35 [kg], corresponding in good approximation to the weight of the liquid N_2 located between the two tops of the tanks have been considered as uniformly spread on the tops themselves. Thus the container tops have been given the properties of a fictitious material

having the same stiffness as anticorodal but such a density (32200 [kg / m^3]) as to get the total mass of the structure itself plus the liquid N_2 35 [kg].

- the remaining 25 [kg] have uniformly been spread on the two container walls. A fictitious material having the same stiffness as anticorodal and a density of 6430 [kg / m^3] (to include both structural mass and liquid N_2) has been introduced to describe them.

The internal container with the liquid He, the optical equipment and the thermal shield have simply been simulated by a point mass of 46 [kg].
Suitable rigid body rotary inertia values, estimated as if all the masses inside the He container were uniformly distributed on its rigid wall, have been assigned to the equivalent point mass.
The distribution of the optical equipment and of the thermal shield masses on the surface of the He container involves an overestimate of the inertia moments in the former case, and an underestimate in the latter, which should at least partially compensate each other from the overall point of view. In any case, in the global economy of the approximations introduced in the model, these further ones don't change the reliability of the model itself for the present scope of the analysis.

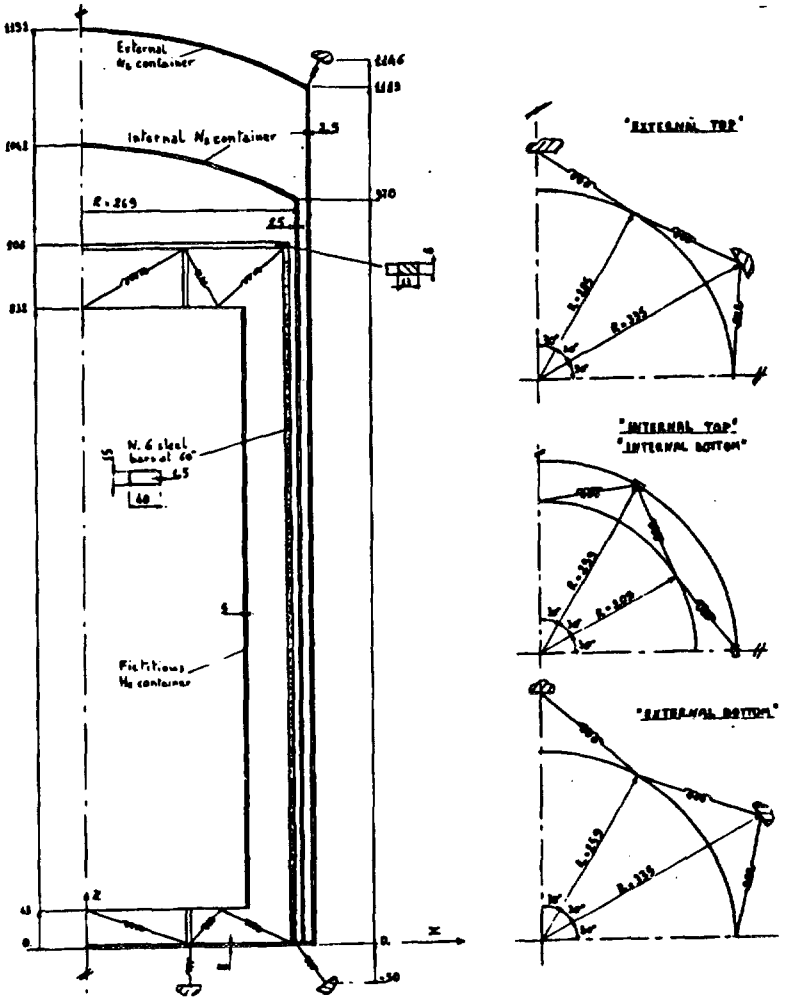

fig. 13

4.2 Finite Element Analysis

The following considerations have carefully been taken into account while realizing the finite element model:

1) The mass of the system is essentially concentrated on the top of the liquid N_2 container and in the point mass simulating all the internal structures (He container, liquid He, thermal shield and optical equipment).

2) The flexibility of the system is mainly located in correspondence of the kevlar cords, and of the six steel beams supporting the He container.

Thus a simple finite element model with its main focus on these points has been set up for the entire structure (see a front view in fig.14) consisting of :

114 quadratic shell elements simulating the internal and external tanks for liquid N_2 and the anticorodal bottom plate;

48 quadratic beam elements simulating the supporting system of the internal structures;

48 linear truss elements simulating kevlar cords;

1 mass and 1 rotary elements simulating the inertial effects of the internal structures.

The model has globally 212 elements, 918 nodes and 4224 degrees of freedom.

The lowest 11 natural frequencies and the corresponding mode shapes have been calculated and verified.

4.3 Results

The results of the analysis are summarized in Tab.3, while the related mode shapes are shown in fig.15.

The 15.5 Hz frequency corresponds to two mode shapes, which exibit a lateral deformation respectively along the y and x axes (because of the symmetry of the model) of the six steel beams supporting He container and optical equipment, as it is confirmed by the value of the effective mass involved in such natural vibration modes.

The third mode (f=16.7 Hz) involves practically all the suspended mass, as if it were a rigid body oscillating vertically along the z axis with the top and bottom kevlar cords, each simulated by 12 springs, as the only flexibility elements in the model. Infact for a mass suspended by a set of different springs we get :

$$f_z = \frac{1}{2\pi}\sqrt{\frac{\sum_i k_i \cos\vartheta_i}{m}}$$ where:

m is the total mass (m=157 [kg]),

$k_i = \frac{E_i A_i}{l_i}$ is the stiffness of the i-th spring,

E is the Young's modulus of kevlar,

A is the cross section area,

l is the spring length,

ϑ is the angle of the cord with the vertical.

By replacing the proper values : $k_z = 1.79 \cdot 10^6$ [N / m] , $f_z \cong 17$ [Hz]

which is ruther close to the value of 16.7 [Hz] calculated by finite element analysis.

The 50.5 [Hz] and 62.9 [Hz] frequencies correspond essentially to two couple of flexural modes (because of symmetry) of the liquid N_2 containers and to a "second vibration mode" of the six steel beams supporting the He container.

As it can be seen from Tab.3, only the modes involving a considerable amount of the effective mass of the structure have been reported while modes from 8 (f=65 [Hz]) to 11 (f=76 [Hz]) have been omitted because the corresponding effective mass is really very negligible. Their

mode shapes are quite unreliable because they concern the ovalization deformation of the ring and of the two liquid N_2 containers which haven't properly been meshed to this aim.
Modes 1, 4, 6 and modes 2, 5, 7 globally involve 97% of the mass in vibrating shapes along the y axis and the x axis respectively, whereas nearly 100% of the effective mass vibration along the z axis is related to the third mode. Among the first 11 modes calculated in the analysis, there has been no evidence of torsional ones. It can be shown by some simple calculations that the related frequencies are higher (see Appendix 1).
As a parametric study, the same eigenvalue extraction has been carried out for the same finite element model with the only variation of kevlar cord diameter. The results relative to kevlar cord diameters D=2.15 [mm] and D=1.6 [mm] are respectively reported in Tab.4 and in Tab.5. The same qualitative considerations apply to these new cases. It is obvious that the reduction of the kevlar cord diameter involves a stiffness decrease responsible for general lower frequency values.

Tab.3

Mode number	Frequency [Hz]	Effective mass [kg]	Direction
1, 2	15.5	45.9	y, x
3	16.7	156.8	z
4, 5	50.5	90.4	y, x
6,7	62.9	16.1	y, x

Tab.4 (kevlar cord D=2.15 mm)

Mode number	Frequency [Hz]	Effective mass [kg]	Direction
1	11.3	156.9	z
2,3	11.4	45.0	y,x
4, 5	36.5	104.6	y, x
6,7	43.3	4.7	y, x

Tab.5 (kevlar cord D=1.6 mm)

Mode number	Frequency [Hz]	Effective mass [kg]	Direction
1	8.4	157	z
2,3	9.1	46	y,x
4, 5	27.8	107	y, x
6,7	32.5	2	y, x

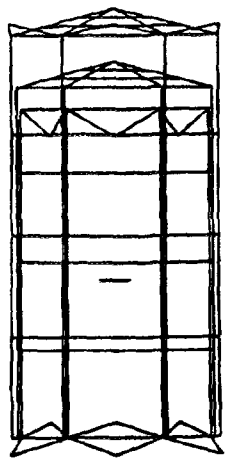

fig.14

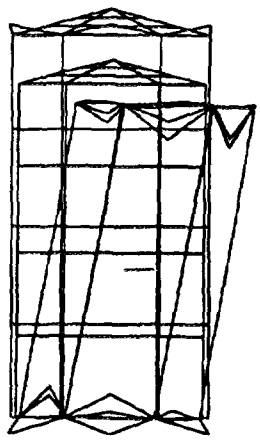

f=15.5 Hz

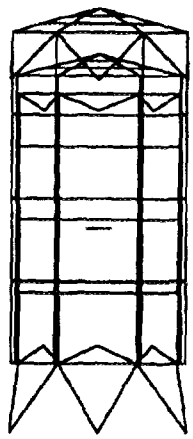

f=16.7 Hz

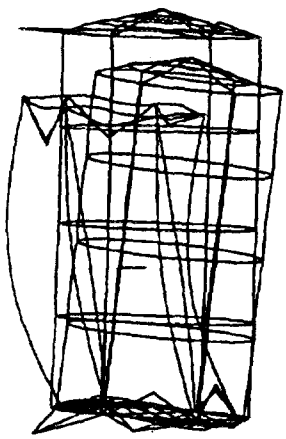

f=50.5 Hz

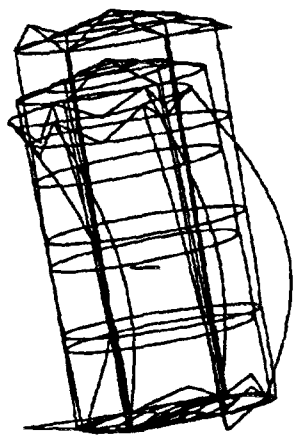

f=62.9 Hz

fig.15

5.0 Modal Analysis of an Alternative Design

Beside the design approach based on kevlar cords, also a different solution for the support system of the cryostat components, consisting of fiber glass cylinders, has been analyzed and its natural frequencies and related mode shapes determined.
The main feature of this design (more complicated and expensive) is the presence of three fiber glass cylinders schematically arranged as shown in fig.16.

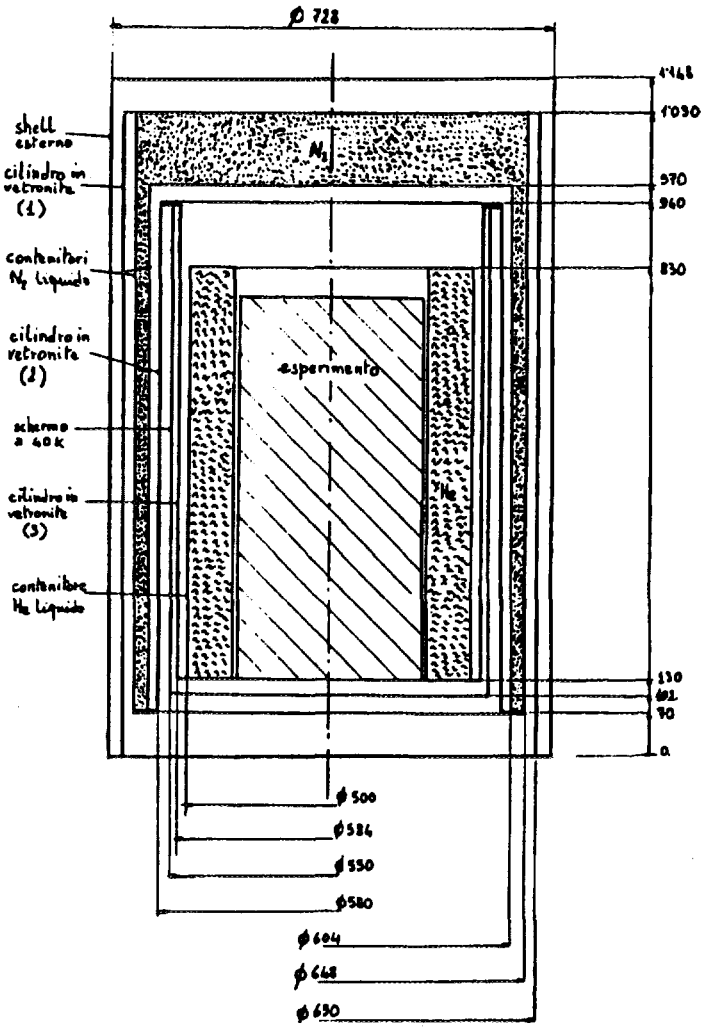

fig. 16

5.1 Input Data and Model

The geometry of the cryostat is different in this case from that of the kevlar design and the dimensions, in [mm], assumed for the modal analysis are shown in fig.16. All the structure is a sequence of nested cylinders. In particular the fiber glass cylinder (3) supports the liquid He container and the optical equipment. The fiber glass cylinder (2) supports the 40 K thermal shield and cylinder (3) by means of a flange at the top. The fiber glass (1) supports the two liquid N_2 containers and cylinder (2), namely all the internal structures.

The material properties are given in 2.3, while weights and thicknesses in the FEM model are:

fiber glass cylilinder (1)	:	5 [kg] , 1 [mm]
fiber glass cylilinder (2), (3)	:	3 [kg] , 0.5 [mm]
anticorodal N_2 containers	:	30 [kg] , 2.5 [mm]
liquid N_2	:	60 [kg]
anticorodal thermal shield	:	3 [kg] , 1 [mm]
He container + liquid He	:	22 [kg] (point mass)
optical equipment	:	15 [kg] (point mass)
anticorodal flanges	:	2 [kg]
Total mass	:	140 [kg]

Liquid N_2 mass has been distributed on the two tanks by following the same method described in 4.1. Thus the container tops have been given the properties of a fictitious material having the same stiffness as anticorodal but such a density (22200 [kg / m^3]) as to include the pertinent liquid N_2 mass. The density of the vertical walls of the two containers has been increased to about 5900 [kg / m^3] for the same reason.

5.2 Finite Element Analysis

The determination of the lowest natural vibration frequencies of the structure has been the goal of the analysis. Not too refined a finite element discretization has been necessary to this aim. The model which has been set up consisted of :

- 528 quadratic shell elements simulating the two tanks for liquid N_2, the thermal shield and the three fiber glass cylinders;
- 48 beam elements simulating the connection flanges;
- two mass elements simulating the inertial properties (mass and inertia moments) about the center of mass respectively of :
  the He container and He itself;
  the optical equipment.

The model has globally 578 elements, 2788 nodes and 14664 degrees of freedom.

5.3 Results

The results of the analysis are summarized in Tab.6.
The 17.6 [Hz] frequency corresponds to two mode shapes, which exibit a lateral deformation respectively along y and x axes (because of the symmetry of the model) of the internal structure, something like a rigid oscillation of all the supported structure about the edge of the main fiber glass cylinder (1), involving about one half of the total mass.
The 19.1 [Hz] frequency corresponds to a vibration mode along the vertical axis z of the top of the outer container of liquid N_2, whereas the 22.4 [Hz] frequency is related to the analogous mode of the top of the inner container of liquid N_2. To understand this mode shape it must be

remembered that the liquid N_2 has been simulated by increased density of the container walls, including the top and bottom plates.
The 36.4 [Hz] frequency corresponds to a vibration mode along the vertical axis z involving about 40% of the total mass.
The 36.8 and 38.7 [Hz] frequencies correspond to mode shapes resembling those related to the 17.6 [Hz] frequency, involving another 36% of the total mass in rigid oscillations of the internal cylinders vith different relative movement.

Tab.6

Frequency [Hz]	Effective mass [kg]	Direction
17.6	79	y, x
19.1	21	z
22.4	9	z
36.4	57	z
36.8	26	y, x
38.7	24	y,x

Moreover the calculation of the natural frequencies of the same structure was performed with the addition of 4 kevlar cords (diameter equal to 2.15 [mm]) arranged as schematically shown in fig.17, in order to stiffen even more the structure.
From the finite element analysis point of view, that involved the introduction of 64 truss elements simulating the kevlar cords.
The results are summarized in Tab.7.
As it could easily be guessed, the frequencies related to vibration modes along the z axis of the tops of the liquid N_2 containers (19 [Hz] and 22 [Hz]) don't change because kevlar cords have no effects on the stiffness of the two tops.

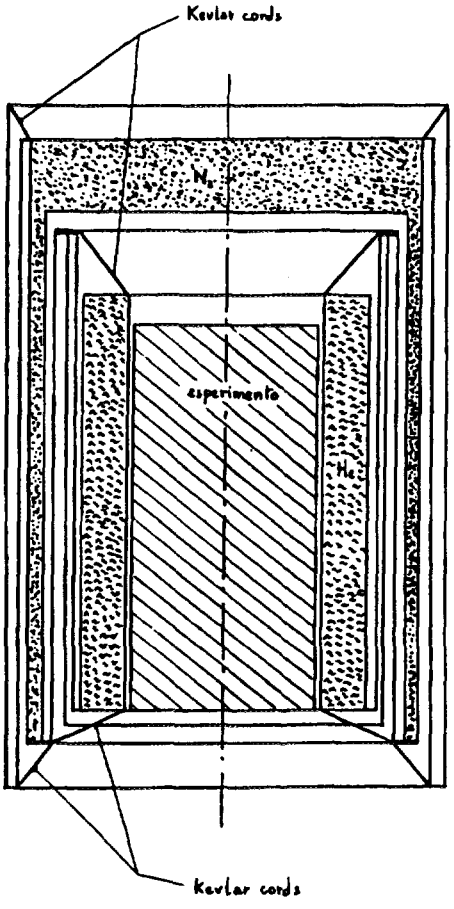

fig. 17

As for the other frequencies it can be noticed there is not only a general shift of the frequency spectrum upwards, but also a different effective mass distribution among the modes. The frequency corresponding to a couple of modes involving a significant effective mass along y, x is now about 33 [Hz] compared to the previous 18 [Hz].
The mode shape revealing a remarkable vibration of the structure along the z axis has now a frequency value of 44 [Hz] compared to the previous 36 [Hz].

Tab.7

Frequency [Hz]	Effective mass [kg]	Direction
19.3	18	z
22.4	9	z
33.1	103	y, x
44.0	66	z

6.0 Conclusions

Several finite element analyses have been performed in order to get useful information required for the design of an adequate cryostat supporting system for the telescope of the BOOMERANG (Ballon Observations Of Millimetric Extragalactic Radiation ANd Geophysics) experiment.
In particular, the calculation of the maximum stresses and deformations in the cryostat supporting system was required in the most severe loading condition, that happens during landing at the time of full parachute opening.
The maximum effects of this dynamic load have been calculated by carrying out a static simulation where the structures are submitted to a gravity load of 10 g.
A parametric analysis has been performed on the model by changing the mesh refinement and some boundary conditions. In all cases the maximum stress values have been found to be quite below the resistence limits of the employed materials.
Modal analysis has been required too in order to get the lowest natural frequency values together with the related mode shapes.
The lowest natural frequencies which have been determined for a 3.2 [mm] diameter of kevlar cords have been found to be about 16 and 17 [Hz]; the former corresponding to a flexural mode of the supporting system of He and optical equipment, the latter to a mode shape involving a vibration along the symmetry axis z.
A parametric study has been carried out by imposing different diameter values for kevlar cords.
Modal analysis has been performed too on an alternative design consisting in a sort of nested cylindrical containers connected at their top or bottom by suitable flange systems with the main supporting function assigned to three fiber glass cylinders.
This design solution is much more complicated and expensive but has been investigated in order to verify if higher frequency values could be obtained. No significant shift upwards of the lowest frequency values has been got with this alternative design.

7.0 References

[1] Lange, A., (California Institute of Technology), De Bernardis, P., De Petris, M., Masi, S.,Melchiorri,F.,(Università La Sapienza), Aquilini, E.,Martinis, L.,Scaramuzzi, F.,(ENEA), Melchiorri, B., (IFA-CNR), Boscaleri, A., (IROE-CNR), Romeo, G., (Istituto Nazionale di Geofisica), Bock, J., Chen, Z., Devlin, M., Gervasi, M., Hristov, V., Mauskopf, P.,Osgood, D., Richards, P., (U.C.B.), Ade, P., Griffin, M., (Queen Mary and Westfield College), "The Boomerang Experiment", Workshop Infrared and Submillimetric Space Missions, Sacley, April 1994 to be published on Space Science Reviews (June 1995).

[2] Hibbitt, Karlsson & Sorensen INC, "ABAQUS", version 5.3

[3] Clough, R.W., Penzien,J.,"Dynamics of structures", Mc Graw Hill, I.S.E.,1975.

[4] Bathe, K.J.,"Finite Element Procedures in Engineering Analysis", Prentice-Hall Inc,1982.

[5] Zienkiewicz, O.C., "The Finite Element Method", 4th ed.,McGraw-Hill Book Co.,1991.

A.1 Approximate Calculations of the Frequency Corresponding to a Torsional Vibration Mode

A first torsional mode can be supposed as a vibration of frequency f_t of all the structure as a rigid body around the z axis (1 dof problem) where all the flexibility is concentrated in the upper and lower kevlar cords supporting the cryostat.
Let's calculate the potential energy E_p of the system, with $E_p = E_{p1} + E_{p2}$, where E_{p1} and E_{p2} are respectively the potential energy of the upper set of 12 springs and of the lower set of 12 springs simulating the kevlar cords, for an infinitesimal relative rotation angle γ about the vertical axis z (fig.A.1) :

$$E_{p1} = 6\left[F_0(l_a - l_0) + \frac{1}{2}k(l_a - l_0)^2\right]_1 + 6\left[F_0(l_b - l_0) + \frac{1}{2}k(l_b - l_0)^2\right]_1$$

$$E_{p2} = 6\left[F_0(l_a - l_0) + \frac{1}{2}k(l_a - l_0)^2\right]_2 + 6\left[F_0(l_b - l_0) + \frac{1}{2}k(l_b - l_0)^2\right]_2$$

or by summarizing :

$$(E_p)_{1,2} = \left[6F_0(l_a - l_0 + l_b - l_0) + 3k(l_a - l_0)^2 + 3k(l_b - l_0)^2\right]_{1,2} \qquad \text{where :}$$

F_0 is the pre-tension in the kevlar cord, that is in each spring;
l_0 is the length of each spring when $\gamma = 0$;
l_a, l_b are respectively the length of two consecutive springs when $\gamma \neq 0$;
k is the spring constant equal to (EA / l_0), where E is the Young's modulus of kevlar and A the cord cross section area.
It can be shown that $(l_a - l_0)$ and $(l_b - l_0)$ (fig.A.1) can be approximated as follows:

$$l_a - l_0 = \frac{rR}{2l_0}\gamma^2 \cos 30° + \frac{rR}{l_0}\gamma \sin 30°$$

$$l_b - l_0 = \frac{rR}{2l_0}\gamma^2 \cos 30° - \frac{rR}{l_0}\gamma \sin 30°$$

By substituting these expressions, we can approximate $(E_p)_{1,2}$ as follows:

$$(E_p)_{1,2} = 6\left[F_0 \frac{rR}{l_0}\cos 30° + k\left(\frac{rR}{l_0}\right)^2 \sin^2 30°\right]_{1,2} \gamma^2$$

The first term in brakets can be neglected compared to the other one. Infact $F_0 = k\,\Delta l_{initial}$ and by taking into account the ratio between these two terms, we have:

$$\frac{F_0 \frac{rR}{l_0}\cos 30°}{k\left(\frac{rR}{l_0}\right)^2 \sin^2 30°} = \frac{2\sqrt{3}\,l_0\,\Delta l_{initial}}{rR} << 1$$

Thus:

$$(E_p)_{1,2} = 6\left[k\left(\frac{rR}{l_0}\right)^2 \sin^2 30°\right]_{1,2} \gamma^2$$

The kinetic energy E_c of the system is given by :

$E_c = \frac{1}{2} I \gamma^2$ where I is the inertia moment of the structure about z.

By applying the Lagrange equation for a 1 dof system, we get:

$$I\ddot{\gamma} + 12\left[\left(k\frac{r^2R^2}{l_0^2}\sin^2 30°\right)_1 + \left(k\frac{r^2R^2}{l_0^2}\sin^2 30°\right)_2\right]\gamma = 0$$

$$I\ddot{\gamma} + k_t\gamma = 0, \quad \text{where} \quad k_t = 3\left[\left(k\frac{r^2R^2}{l_0^2}\right)_1 + \left(k\frac{r^2R^2}{l_0^2}\right)_2\right]$$

By inserting all the numerical values we get :

$$k_t = 3EAR^2\left[\left(\frac{r^2}{l_0^3}\right)_1 + \left(\frac{r^2}{l_0^3}\right)_2\right] = 3 * 29\cdot 10^9 * 8\cdot 10^{-6} * 0.335^2\left[\frac{0.285^2}{0.170^3} + \frac{0.259^2}{0.178^3}\right]$$

$$= 2.22\cdot 10^6 \ [\mathrm{N\cdot m}]$$

The inertia moment I calculated by ABAQUS is : $I = 8.7 \ [\mathrm{N\cdot m}]$

So, finally, the first torsional mode has an estimated frequency : $f_t = \frac{1}{2\pi}\sqrt{\frac{k_t}{I}} = 80 \ [\mathrm{Hz}]$

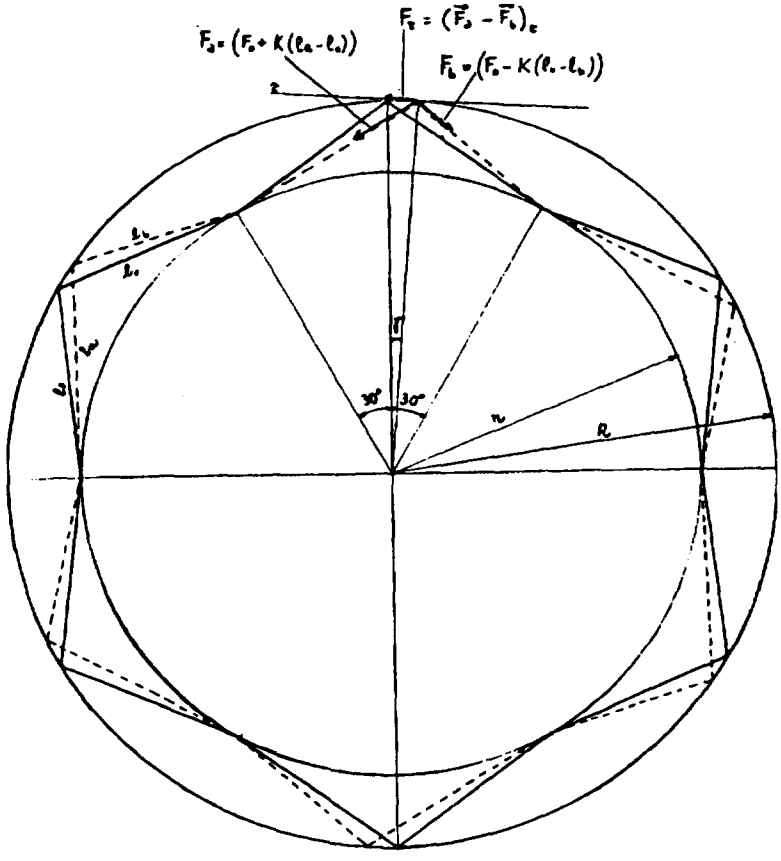

fig. A.1

Edito dall'Enea
Funzione Centrale Relazioni Esterne
V. le Regina Margherita, 125 - 00198 Roma
Finito di stampare nel mese di dicembre 1995
presso il Tecnografico